

International Conference on Space Optics—ICSO 2014

La Caleta, Tenerife, Canary Islands

7–10 October 2014

Edited by Zoran Sodnik, Bruno Cugny, and Nikos Karafolas



A multiple functional connector for high-resolution optical satellites

Fengke She

Gangtie Zheng



icso proceedings



A MULTIPLE FUNCTIONAL CONNECTOR FOR HIGH-RESOLUTION OPTICAL SATELLITES

Fengke SHE¹, Gangtie ZHENG².

School of Aerospace, Tsinghua University, Beijing, China^{1,2}

sherkfung@gmail.com¹

gtzheng@tsinghua.edu.cn²

I. INTRODUCTION

For earth observation satellites, perturbations from actuators, such as CMGs and momentum wheels, and thermal loadings from support structures often have significant impact on the image quality of an optical. Therefore, vibration isolators and thermal deformation releasing devices nowadays often become important parts of an image satellite. However, all these devices will weak the connection stiffness between the optical instrument and the satellite bus structure. This will cause concern of the attitude control system design for worrying about possible negative effect on the attitude control. Therefore, a connection design satisfying all three requirements is a challenge of advanced image satellites.

Chinese scientists have proposed a large aperture high-resolution satellite for earth observation. To meet all these requirements and ensure image quality, specified multiple function connectors are designed to meet these challenging requirements, which are: isolating vibration, releasing thermal deformation and ensuring whole satellite dynamic properties [1].

In this paper, a parallel spring guide flexure is developed for both vibration isolation and thermal deformation releasing. The stiffness of the flexure is designed to meet the vibration isolation requirement. To attenuate vibration, and more importantly to satisfy the stability requirement of the attitude control system, metal damping, which has many merits for space applications, are applied in this connector to provide a high damping ratio and nonlinear stiffness. The capability of the connector for vibration isolation and attenuation is validated through numerical simulation and experiments. Connector parameter optimization is also conducted to meet both requirements of thermal deformation releasing and attitude control. Analysis results show that the in-orbit attitude control requirement is satisfied while the thermal releasing performance is optimized. The design methods and analysis results are also provided in the present paper.

II. CONNECTOR DESIGN

A. Vibration isolation design

The main vibration sources on the satellite bus has been determined as the Control Moment Gyro (CMG). The perturbation frequency is 158 Hz (due to 9000 rpm) and 66 Hz (due to 0.4 rotating speed), the 1st frequency of the satellite with bus directly connected to telescope is about 42 Hz. On the other hand, the 1st frequency of the vibration system should be designed to avoid the 1st frequency of solar array's bending mode, which is 1 Hz.

According to these conditions, the 1st frequency of the vibration isolation system connected to telescope is designed to locate in 5~12 Hz, while the amplify ratios at 66 Hz and 158 Hz should be less than 0.2. The vibration isolation connector is designed as a parallel spring guide flexure [2], as shown in Fig. 1, to satisfy the confined space and thermal stress releasing requirements.

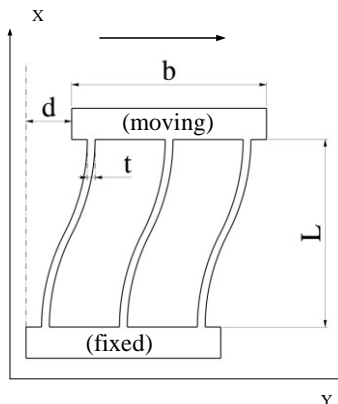


Fig. 1. Parallel spring guide flexure

The stiffness of parallel spring guide flexure at the end of the cantilever along with the motion direction (which is y direction) is given by

$$K_y = \frac{nEt^3L_0}{LL^3} \quad (1)$$

Where K_y is the stiffness of the flexure along with the moving direction, d is the translation motion, L_0 is the blade width, t is the blade thickness, L is the blade length, E is elastic modulus of the flexure material and n is the number of flexure blades.

The stiffness of the flexure at the direction perpendicular to both moving and blade width direction (which is z direction) is given by

$$K_z = \frac{ntL_0G}{L} \quad (2)$$

And G is the shear modulus of the flexure material. The stiffness of the flexure at the blade length direction (which is x direction) is given by

$$K_x = \frac{nEtL_0}{L} \quad (3)$$

Vibration isolation connectors are equally spaced along with the primary mirror mount outer edge. The stiffness of the vibration isolation system is determined as

$$\tilde{K}_x = \tilde{K}_y = 1.5(K_y + K_z) \quad (4)$$

where \tilde{K}_x is the stiffness in x direction and \tilde{K}_y is the stiffness in y direction. With above equations, the fundamental frequencies of the flexure-mounted telescope can be estimated by

$$\tilde{f}_x = \tilde{f}_y = \frac{1}{2\pi} [1.5(K_y + K_z)]^{1/2} \quad (5)$$

where \tilde{f}_x , \tilde{f}_y are the fundamental frequencies in x and y directions, respectively, and m is the telescope mass.

B. Damping design

Considering the in-orbit environment, such as vacuum, extremely high or low temperature, space radiation, and the reliability of the connector, metal damping material are the most ideal material to provide damping to the connector ([3], [4]).

Two types of metal damping elements are made to apply in the connector system. Ring metal rubbers are used between the end of flexure and the telescope mount, as shown in Fig. 2.

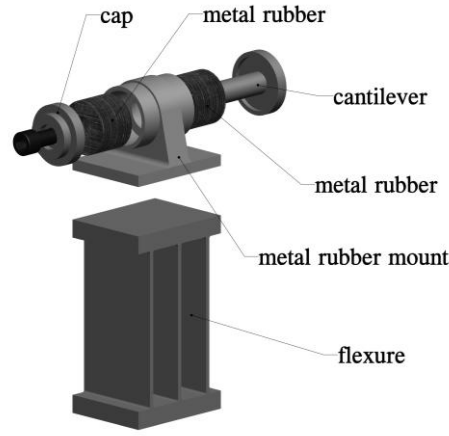


Fig. 2. Damping design

Sheet metal damping elements are combined with flexure blades to provide damping effect when the flexure blades bend.

Due to the damping system requirements, the damping ratio of the damping system should be no less than 14 Ns/m. Experiments are conducted in the future section to validate the effectiveness of the damping system.

C. Thermal deformation releasing design

The parallel spring guide flexure is also used as the device for releasing the thermal deformation. As shown in section 3.1, the stiffness of the flexure along with motion direction is given by

$$K_y = \frac{nEL_0t^3}{L} \quad (6)$$

And the stiffness of the flexure at the blade width direction is given by

$$K_z = \frac{ntL_0G}{L} = \frac{nEL_0t^3}{2(1+\gamma)L} \quad (7)$$

where γ is the Poisson ratio of the flexure material. The entirety stiffness of the connector system is given by

$$\tilde{K}_x = \tilde{K}_y = 1.5(K_y + K_z) \quad (8)$$

In most condition, which means L is much larger than t , and $t \ll L$, so

$$K_z = \frac{1}{2(1+\gamma)} \frac{L^2}{t^2} K_y \gg K_y \quad (9)$$

And

$$\tilde{K}_x = \tilde{K}_y \approx 1.5K_z \quad (10)$$

It is shown that: when t and L_0, L , is determined, thermal release feature improves with the thickness of blades: t decreases and the number of blades: n increases. Meanwhile, the entirety stiffness of the connector system is maintained with little changes in K_z .

However, the thickness cannot be limitless thin due to the reliability and manufacture issue. With all this conditions considered and simulation conducted, n is chosen to be 3, and t is 2 mm.

II. SIMULATION AND EXPERIMENTS

A. Vibration isolation simulation

In this section, the connector system's effectiveness for vibration isolation is validated through simulation using both rigid body model and satellite entirety model.

For preliminary analysis, telescope and satellite bus are modeled as rigid body. The finite element model is shown in Fig. 3 and the first 6 modal frequencies are given in Table. 1.

The requirement that the fundamental modal frequency must be in 5~12 Hz is satisfied. The amplify ratio at 66 Hz and 158 Hz at Rx-Rx and Ry-Ry directions are shown in the Fig. 4.

Since Rx and Ry directions are the most concerned directions, which the transfer ratio at these two directions effect the image quality most. It is shown that the amplify ratios at both sensitive direction are less than 0.2 and satisfied the vibration isolation requirements.

The finite element model of the connector system connected to telescope is shown in Fig. 5.

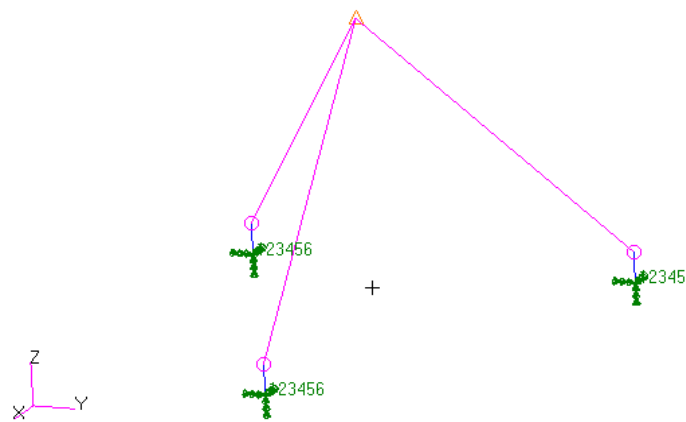


Fig. 3. Point mass model

Table. 1. The first 6modal frequencies

Level	Frequency (Hz)	Modal description
1	9.15	Rotation in x direction (Rx)
2	10.41	Rotation in y direction (Ry)
3	19.76	Rotation in z direction (Rz)
4	26.28	Translation in x direction (Tx)
5	27.18	Translation in y direction (Ty)
6	27.86	Translation in z direction (Tz)

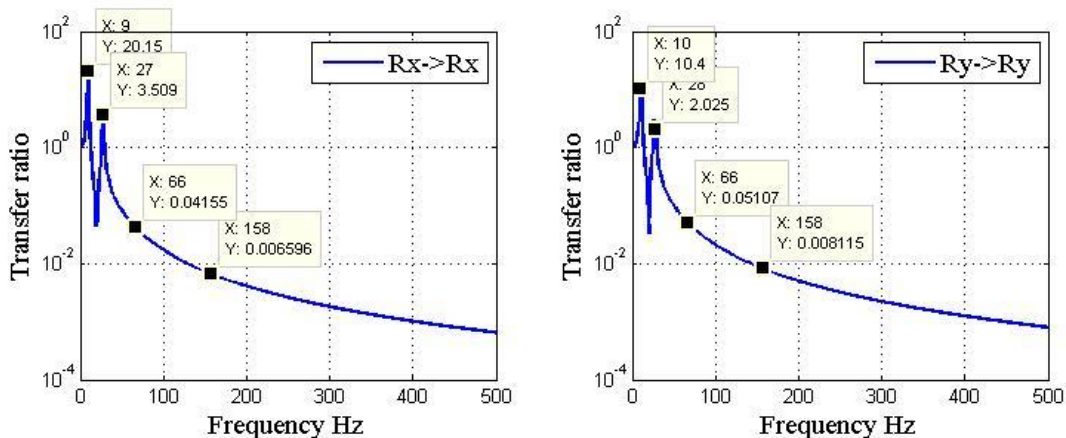


Fig. 4. The transfer function at Rx-Rx and Ry-Ry directions



Fig. 5. Telescope finite element model

The finite element model of the satellite bus and telescope combined with connector system is shown in Fig. 6.

The transfer function from CMG to the primary mirror mass point (of both Rx and Ry direction) is shown in Fig. 7.

The transfer ratio from CMG to the primary mirror mass point (of both Rx and Ry direction) is given in Table. 2.

The simulation shows that: on the most concerned directions, i.e. Rx and Ry, the transfer ratios of perturbation are most below 0.3, even on those not so satisfied directions, future analysis proved that the vibration at the mirror mass point is much smaller than other directions.

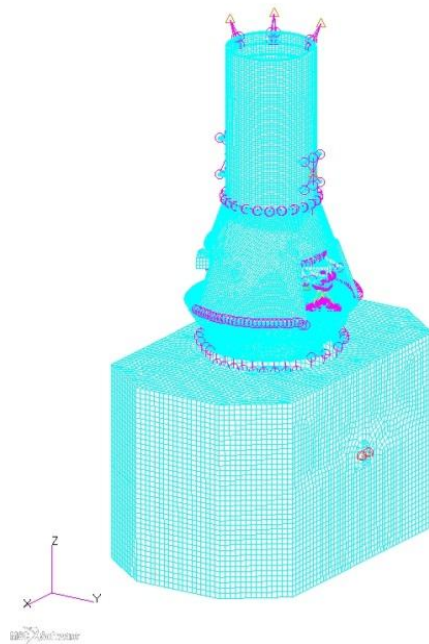


Fig. 6. The finite element model of the whole satellite

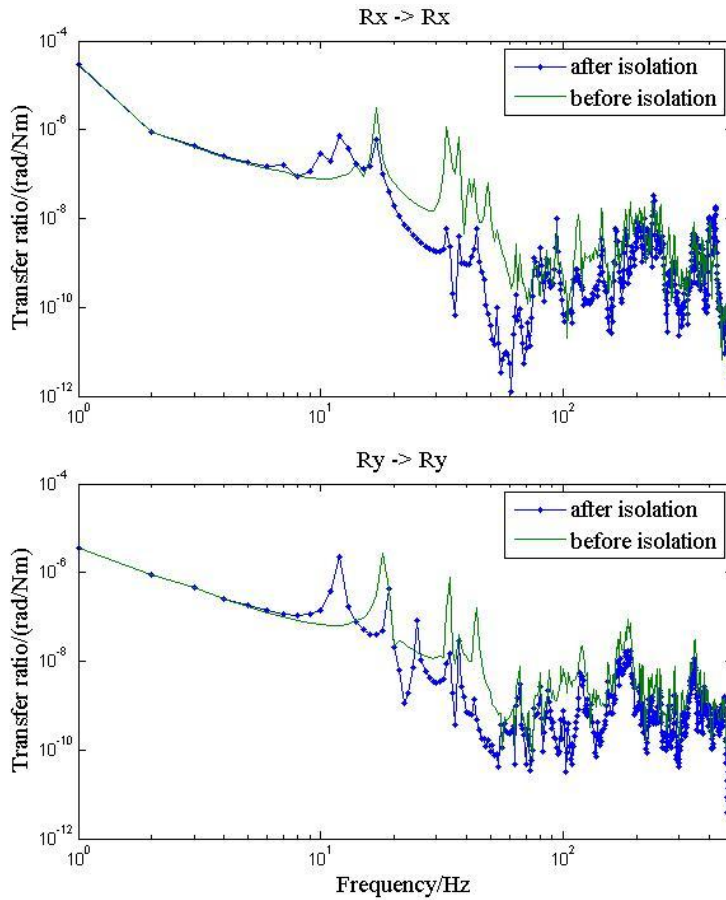


Fig. 7. The transfer function from CMG to the primary mirror mass point

Table. 2. The transfer ratio from CMG to the primary mirror mass point

Directions	Transfer ratio at 66 Hz		Transfer ratio at 158 Hz	
	Rx	Ry	Rx	Ry
1	0.08	0.25	0.38	0.65
2	0.15	0.24	0.79	0.48
3	0.09	0.25	0.89	0.72
4	0.07	0.26	0.09	0.38
5	0.06	0.26	0.22	0.35
6	0.02	0.12	0.31	0.21

B. Damping experiment

Though many researches have been conducted to study the damping force of metal rubber, still it is difficult to determine metal rubber's damping force theoretical. Thus, specified experiments are conducted to measure damping ratio of the ring metal rubber. The whole measure system is shown in Fig. 8.

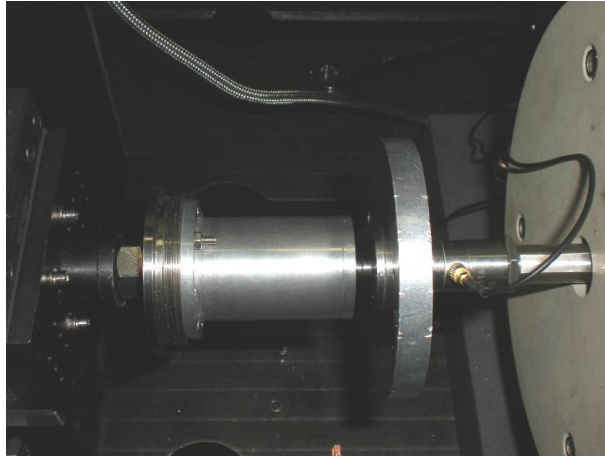


Fig. 8. Damping measure system

The ring metal rubber are fixed to measuring force platform at one end and at another end to vibration exciter. The damping ratio of metal rubber can be calculated with the measured response force, exciting force and metal rubber velocity. The experiment result shows the damping ratio of the damping element is up to 53 Ns/m, satisfies the required damping ratio 14 Ns/m.

C. Thermal deformation releasing simulation

The RMS of the satellite primary mirror deformation under extremely temperature condition are calculated to validate the effectiveness of the connector system thermal releasing feature. The finite element model of primary mirror is shown in Fig. 9.

Temperature gradient of 60K (from 263K to 327K) on three directions: x, y ,z are applied on the satellite finite element model. The RMSs of mirror surface deformation before and after deformation released are given in Table. 3.

The thermal releasing simulation result shows that: the connector system functions well to release the thermal deformation applied on the primary mirror from satellite bus.

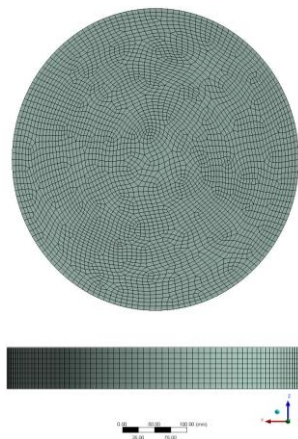


Fig. 9. Primary mirror finite element model

Table. 3. The RMSs of mirror surface deformation

Gradient direction	After released (nm)	Before released (nm)	Residual
X	17	51	0.34
Y	25	88	0.28
Z	251	1160	0.22
Both X and Z	265	1159	0.23

III. CONCLUSION

In this paper, a multiple functional connector is designed to isolate the micro-vibration from CMGs, release the thermal stress from satellite bus while the requirement of the satellite entirety dynamic property is satisfied. Results show that the multiple function connector system satisfactorily meets all requirements.

REFERENCES

- [1] Zhichun SHEN, Lu LIANG, Gangtie ZHENG, Jiangang ZHANG, Xiaoying MAN, Lamei CHE. Vibration suppression of a payload bracket in a satellite [J]. *Journal of Astronautics*, 2005, 27(3): 503-506.
- [2] Vukobratovich, Daniel, and Ralph M. Richard. "Flexure mounts for high-resolution optical elements." 1988 Dearborn Symposium. International Society for Optics and Photonics, 1988.
- [3] Jiamin WANG, Tingguo PEI, Theory and experiment research on a new type of metal rubber damper for inertial platform [J], *Journal of Astronautics*, 2003, 24(1): 92-96.
- [4] Minghui LIU, Lu Liang, Shaojun BAI, Jing ZHANG, Gangtie ZHENG, Research into the integrative Application of Damped Flexible Connector in Spacecraft Structures [J], *Journal of Astronautics*, 2009, 30(1), 293-298.